Vol 11 No 10, October 2002
1009-1963/2002/11(10)/1037-05

Chinese Physics

© 2002 Chin. Phys. Soc.
and IOP Publishing Ltd

Small angle x-ray scattering study on the conformation of polystyrene in toluene during adding anti-solvent CO_2

Liu Yi(柳 义)[a], Chen Dong-Feng(陈东风)[a], Wang Hong-Li(王洪立)[a], Chen Na(陈 娜)[a], Li Dan(李 丹)[b], Han Bu-Xing(韩布兴)[b], Rong Li-Xia(荣利霞)[c], Zhao Hui(赵 辉)[c], Wang Jun(王 俊)[c], and Dong Bao-Zhong(董宝中)[c]

[a] *China Institute of Atomic Energy, Beijing* 102413, *China*
[b] *Institute of Chemistry, Chinese Academy of Sciences, Beijing* 100080, *China*
[c] *Institute of High Energy Physics, Chinese Academy of Sciences, Beijing* 100039, *China*

(Received 18 March 2002; revised manuscript received 15 May 2002)

The conformation of polystyrene in the anti-solvent process of supercritical fluids (compressed CO_2 + polystyrene + toluene) has been studied by small angle x-ray scattering with synchrotron radiation as an x-ray source. Coil-to-globule transformation of the polystyrene chain was observed with the increase of the anti-solvent CO_2 pressure; i.e. polystyrene coiled at a pressure lower than the cloud point pressure (P_c) and turned into a globule with a uniform density at pressures higher than P_c. Fractal behaviour was also found in the chain contraction, and the mass fractal dimension increased with increasing CO_2 pressure.

Keywords: small angle x-ray scattering, supercritical fluid, anti-solvent process, polystyrene
PACC: 6110, 6140

1. Introduction

The anti-solvent process of supercritical fluids has been becoming more and more attractive in the fields of chemical industry and materials science.[1−6] The basis of the gaseous anti-solvent (GAS) technique[7] is that the supercritical fluids in a dense gas state are generally soluble in organic solvents and in the solution of these solvents with crystallizable solutes. The dissolution of the GAS causes a volumetric expansion of the solvent and lowers its solvent power, thus forcing the solutes to precipitate. In the process, the properties of the products, such as particle shape, size distribution and morphology, etc, can be tuned by pressure, temperature and concentration of the solutes, and the solvent-free products can be obtained by extracting all of the solvent in the gas phase. To date, the GAS technique has been successfully used in recrystallization of organic solids,[5] fractionation of natural products,[6] and preparation of ultra-fine particles,[1−4] including polymer microparticles.[2−4] It is obvious that the investigation of the effect of the GAS on polymer conformation is of both theoretical and practical importance.

Small angle x-ray scattering (SAXS), which is caused by a spatial fluctuation of the electronic density within a material, is a powerful tool for studying nanoscale materials,[8] so it is an ideal method for the study of the conformation of polymer chains.[9] By using synchrotron radiation as the x-ray source, which has the advantages of high intensity and narrow angular divergence over conventional x-ray generators, one can increase the resolving power and decrease the experiment time, thus enhancing the efficiency of the experiment and expanding the range of application of SAXS to a great extent. In this paper, we report on the SAXS study of the conformation of a polymer chain in the solution (polystyrene + toluene) during the addition of anti-solvent CO_2. The study of the phase change of the polymer chain in the anti-solvent process of supercritical fluids by SAXS has not yet been reported, as far as we know.

2. Theory

In the SAXS theory, the structural information of the scatterer is contained in the scattering curve. Supposing the scattering intensity is $I(h)$, h is the scattering vector, $h = 4\pi \sin\theta/\lambda, 2\theta$ is the scattering angle, λ is the incident x-ray wavelength, some structure parameters can be obtained after the data treatment and analysis of the $I(h)$–h curve.

2.1. Particle size and radius of gyration

The particle size distribution in a polydisperse system can be determined through the following equation

$$I(h) = A\int_0^\infty N(R)R^6 I_0(hR)\mathrm{d}R, \tag{1}$$

where A is a constant, $N(R)$ is the distribution function, R is the radius of a particle, and $I_0(hR)$ is the normalized scattering intensity of a single particle. The distribution function $N(R)$ can be obtained by the fit of scattering intensity in Eq.(1) with the data from experiments. After discretization of Eq.(1), the least-squares method is carried out by step-wise regression analysis. By minimizing the sum of squared differences of the residuals, the discrete value of $N(R)$ and the average value of particle radius are determined.

The average size of particles can also be characterized by the radius of gyration. This is obtained from Guinier's law that the state scattering intensity $I(h)$ should comply with the following equation at small values of h

$$I(h) = I_0\exp\left(-\frac{1}{3}R_\mathrm{g}^2h^2\right), \tag{2}$$

where I_0 is a constant, and R_g is the radius of gyration. By taking a natural logarithm of Eq.(2), the average value of R_g^2 (polydisperse system) can be determined from the slope of the linear part of the $\ln I(h)$–h^2 curve.

As for spherical particles, the following relation holds

$$\overline{R}_\mathrm{g} = \sqrt{3/5}\overline{R}, \tag{3}$$

where $\overline{R}_\mathrm{g}$ and $\overline{R}$ are the average values of R_g and R, respectively.

2.2. Porod's law and its deviation

Porod's law means that for an ideal two-phase structure with sharp and smooth phase boundaries, the asymptotic behaviour of the scattering intensity at large values of h, as shown by curve 1 in Fig.1, is found to be

$$\lim_{h\to\infty}[h^4\cdot I(h)] = K, \tag{4}$$

where K is a constant.

In some cases, negative and positive deviations from Porod's law occur (shown by curves 2 and 3 in Fig.1). The negative deviation is attributed to the existence of a diffuse boundary between two phases, and the positive deviation to the fluctuation of the electron density of any phase.

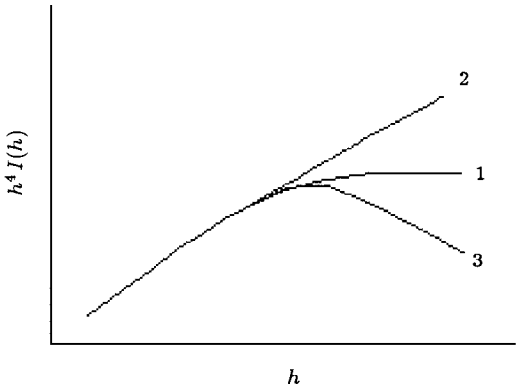


Fig.1. Porod's curve: 1, no deviation; 2, negative deviation; 3, positive deviation.

2.3. Fractal analysis

The concept of fractal geometry is a useful tool to describe a random or disordered system. Qualitatively, fractal objects show dilation symmetry, meaning that the essential geometric features are invariant to scale changes. In the behaviours of SAXS, fractals show a power-law dependence of the scattering intensity[10–11]

$$I(h) = I_0h^{-\alpha}, \tag{5}$$

where α is a constant with its value lying between 0–4, with $3 < \alpha < 4$ for surface fractals, the fractal dimension $D = 6-\alpha$, and with $0 < \alpha < 3$ for mass fractals, $D = \alpha$. Thus, by plotting $\ln I(h)$ versus $\ln h$, one may determine either the surface fractal or mass fractal, if there is a linear region on the scattering curve, and further obtain the fractal dimension.

3. Experiments

3.1. Materials

CO_2 (>99.995% purity) was provided by the Analysis Instrument Factory of Beijing. Polystyrene (PS) (M_w=7.8×10^4, $M_\mathrm{w}/M_\mathrm{n}$=1.1) was supplied by the State Key Laboratory of Polymer Science, Institute of Chemistry, Chinese Academy of Sciences. Toluene (A. R. grade) was produced by the Beijing Chemical Factory. The PS/toluene solution with a concentration of 4.6×10^{-4}g·cm^{-3} was prepared by the gravimetric method.

3.2. SAXS experiments

The high-pressure SAXS cell was made of stainless steel with two diamond windows of 8mm diameter and 0.4mm thickness so as to allow the x-ray to come through. The cell body was coiled with an electric

heater and heat-insulated ribbon. There was a small magnetic stirrer in the cell to stir the fluids before the SAXS measurements, so that the equilibrium could be reached in a short time. The cell could be electrically heated to a certain temperature using a temperature controller with a platinum resistance temperature probe (model XMT, produced by Beijing Chaoyang Automatic Instrument Factory).

Before the experiment, the SAXS cell was filled with a suitable amount of PS/toluene solution at 308.15K, then CO_2 was charged into the cell by a high-pressure pump at a desired pressure while stirring. The cell was connected to the SAXS apparatus after the equilibrium was reached.

The SAXS experiment was performed using synchrotron radiation as the x-ray source with the point-like collimation system at the Beijing Synchrotron Radiation Laboratory.[12] The incident x-ray wavelength λ was 0.154nm, and the scattering angle 2θ was approximately $0^\circ - 3^\circ$. The scattered x-ray intensities were recorded by using image plate technology. The experimental data were treated by a program written in FORTRAN language after subtracting the scattering of solvent and background.

4. Results and discussion

4.1. Size

In the experiment, CO_2 was charged into the cell at pressures of 1.5, 2.4, 3.3, 4.2 and 4.9MPa. Guinier's curves of PS at different pressures are shown in Fig.2. It is seen that the slope of the curve in the region of small values of h decreases as the pressure increases.

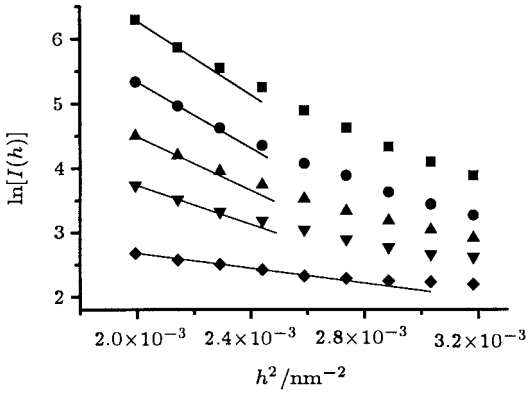


Fig.2. Guinier's curves of PS at different pressures: ■, 1.5MPa; ●, 2.4MPa; ▲, 3.3MPa; ▼, 4.2MPa; ◆, 4.9MPa.

This indicates that the radius of gyration of PS decreases with increasing CO_2 pressure, and that there is an apparent linear part on the curve at a pressure of 4.9MPa, showing that the particles in the liquid are in a narrow size distribution. The average radii of gyration, R_g of PS determined from the curves through Eq.(2) are listed in Table 1. The average radii, R, determined from Eq.(1) and the average radii of gyration, R'_g, determined from Eq.(3) by using the known value of R are also listed in the table.

Table 1. Average radii of PS at different pressures.

Pressure/MPa	R/nm	R_g/nm	R'_g/nm
1.5	9.8	9.3	7.6
2.4	9.2	8.7	7.1
3.3	8.8	7.8	6.8
4.2	7.7	6.9	6.0
4.9	4.6	3.9	3.6

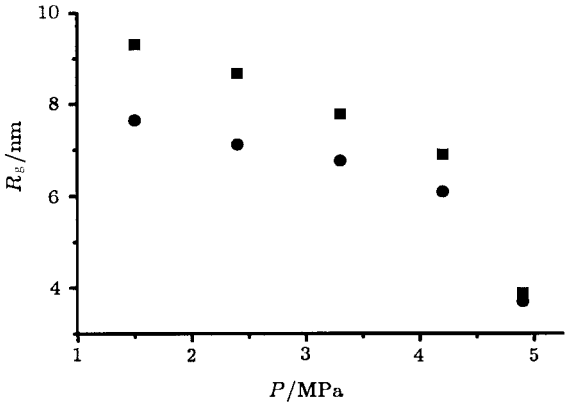


Fig.3. The relation of the average radius of gyration of PS versus pressure: ■, from Eq.(1); ●, from Eq.(2).

Table 1 shows that the average size (whether the radius, or the radius of gyration) of PS decreases with the increase of CO_2 pressure, and that the difference between the values of R_g and R'_g becomes less and less as the pressure increases; they are quite close to each other at a pressure of 4.9 MPa (Fig.3). We know that CO_2, as an anti-solvent gas dissolved in PS/toluene solution, can expand the volume of the solvent and lower its solvent power, and that the conformation of the polymer chain depends on solvent quality, i.e. the coil expands in a good solvent due to its prevailing intersegmental repulsion and contracts in a poor solvent due to its prevailing intersegmental attraction. Toluene is a good solvent for PS, so the chains experience shrinking in the course of adding anti-solvent CO_2. The comparatively greater differences between R_g and R'_g at pressures lower than the cloud point pressure (P_c) suggest a deviation of the spherical particle model from the true PS chain. But PS is quite

close to a spherical particle at pressure higher than P_c, when it is precipitated in particles. P_c, defined as the pressure at which the polymer begins to precipitate, was found to be 4.77 MPa from the further phase equilibrium experiment in which the precipitates in a solution could be seen when P_c was reached. Phase separation occurs when the anti-solvent CO_2 pressure is higher than P_c. It is reasonable that the precipitated particles are in a narrow size distribution if the high and uniform degree of supersaturation is considered.

4.2. Porod's deviation

Figure 4 shows Porod's curves at different CO_2 pressures. It can be found that positive deviations from Porod's law occur at pressures lower than P_c, and that scattering intensity only conforms to Porod's law at pressures higher than P_c. The change of Porod's curves means that PS is of coiled irregular chains in solution and has an uneven density at pressures lower than P_c. These coiled irregular chains turn into spherical particles of uniform density with sharp smooth phase boundaries at pressures higher than P_c.

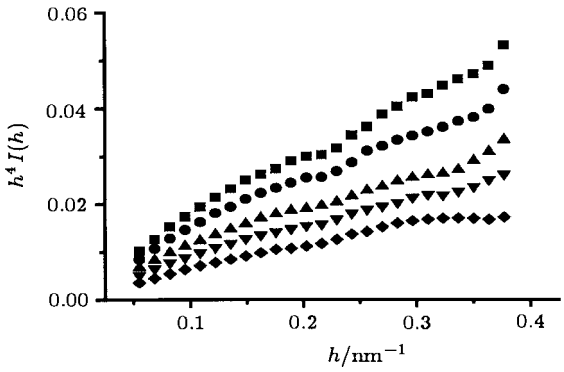


Fig.4. Porod's curves of PS at different pressures: ■, 1.5MPa; ●, 2.4MPa; ▲, 3.3MPa; ▼, 4.2MPa; ◆, 4.9MPa.

4.3. Fractal behaviour

Figure 5 shows the double-logarithmic curve of $I(h)$ versus h at a CO_2 pressure of 1.5MPa. There is an apparent linear part on the scattering curve in the plot, indicating that PS chains have a fractal structure. Further analysis verifies that it is mass fractal. Very similar behaviours are found at other pressures, but the slope of the linear part depends largely on the pressure. Fractal dimensions of D are 2.49, 2.61, 2.71, 2.79 and 2.92 for pressures of 1.5, 2.4, 3.3, 4.2 and 4.9MPa, respectively. A fractal dimension between 2.49–2.92 is characteristic of a polymer chain that has an internal structure between a hard sphere (D=3.0) and a fully swollen randomly coiled macromolecule in a thermodynamically good solvent (D=2.0).[13] The fractal dimension is a measure of the compactness of a polymer chain. The larger the fractal dimension, the more compact the structure is, and the lower the fractal dimension, the more open the structure is. As can be seen, the fractal dimension increases with increasing CO_2 pressure, indicating a collapse of polymer chains from a coil to rather dense globule form in the course of adding anti-solvent CO_2.

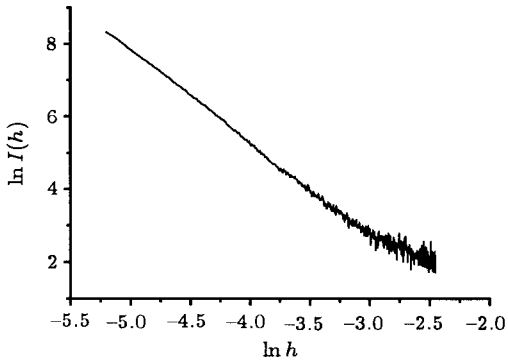


Fig.5. Double-logarithmic curve of $I(h)$ versus h for PS at a pressure of 1.5MPa.

5. Conclusion

With synchrotron radiation as an x-ray source, SAXS was used to study the conformation of PS in the anti-solvent process of supercritical fluids. The results have been summarized after the data treatments and analyses. The solvation power of a solvent decreases during adding anti-solvent CO_2 and, accordingly, the size of PS chains decreases in the process; i.e. they contract at pressures lower than the cloud point pressure (P_c) and turn into particles with uniform density and sharp smooth boundaries at pressures higher than P_c. Fractal behaviour is found in the contraction, and the mass fractal dimension increases with increasing anti-solvent CO_2 pressure.

References

[1] Reverchon E, Porta D G, Sannino D and Ciambelli P 1999 *Powder Technol.* **102** 127

[2] Mawson S, Johnston K P, Betts D E *et al* 1997 *Macromolecules* **30** 71

[3] Luna-Barcenas G, Kanakia S K, Sanchez I C *et al* 1995 *Polymer* **36** 3173

[4] Yeo S D, Debenedetti P G, Radosz M *et al* 1995 *Macromolecules* **28** 1316

[5] Gallagher P M, Coffey M P and Krukonis V J 1992 *J. Supercrit. Fluids* **5** 130

[6] Catchpole O J, Hochmann S and Anderson S R 1996 *High Press. Chem. Eng.* **309**

[7] Guinier A and Fowrnet G 1955 *Small-Angle X-ray Scattering* (New York: Wiley)

[8] Smith T and Carpenter D K 1968 *Macromolecules* **1** 204

[9] Mandelbrot B B 1982 *The Fractal Geometry of Nature* (New York: Freeman)

[10] Bale H D and Schmidt P W 1984 *Phys. Rev. Lett.* **53** 596

[11] Li Z H, Sun J H, Zhao J P *et al* 2000 *Acta Phys. Sin.* **49** 775 (in Chinese)

[12] Dong B Z, Sheng W J, Yang H L and Zhang Z J 1997 *J. Appl. Crystallogr.* **30** 877

[13] Stauffer D, Coniglio A and Adam M 1982 *Adv. Polym. Sci.* **44** 103